

Aqueous Extract of Ginger as Green Corrosion Inhibitor for Mild Steel in Hydrochloric Acid Solution

M.M.B.El-Sabbah^{1*}, H.F.Y.Khalil¹, M.H.Mahross², B.N.A.Mahran³, A.Z. Gomaa⁴,

1- Chemistry Department Faculty of Science, Al-Azhar University, Nasr City, Cairo, Egypt

2-Chemistry Department Faculty of Science, Al-Azhar University, Assiut, Egypt

3-Laboratory for Environment Quality Monitoring, National Water Research Center, Egypt.

4-Paint Consultant

* E-Mail: mmbel_sabbah@hotmail.com

Abstract: The aqueous extract of ginger (AEG) has been studied as a possible source of green inhibitor for corrosion of mild steel in 1 M HCl at temperature range 25-55o C using the conventional weight loss, Open circuit potential (OCP) , linear and Tafel polarization techniques. The evaluation of extract of ginger against different microorganisms has also been providing by using biocide. Moreover the structure of aqueous extract of ginger is analyzed by GC-MS spectra. The inhibition efficiency was found to increase with increasing concentration of the inhibitor and with decreasing temperature. The adsorption of aqueous extract of ginger on the mild steel surface obeys the Langmuir adsorption isotherm. Polarization studies indicate that the aqueous extract of ginger is mixed type inhibitor. The thermodynamic functions of adsorption processes were calculated from weight loss at different temperatures data and were used to analyses the inhibitor mechanism. The surface morphology of the mild steel specimens was evaluated using SEM and EDAX analysis.

Keywords: aqueous extract of ginger, mild steel, inhibitors, surface morphology.

Corresponding author-mail address: mmbel_sabbah@hotmail.com

1-INTRODUCTION

In recent years, owing to the growing interest and attention of the world towards the protection of the environment and the hazardous effects of using chemicals on the ecological balance, the traditional approach on corrosion inhibitors has gradually changed. For an inhibitor to be an effective protector against metal corrosion, it should be readily adsorbed on the metal surface through either physisorption or chemisorption processes. Either of these adsorption processes depends primarily on the physicochemical properties of the inhibitor group such as functional groups, electronic density at the donor atom, molecular structure, etc. For instance, organic molecules, which have had a wide applicability and that have been extensively studied and used as corrosion inhibitors, often contain nitrogen, oxygen, and sulfur atoms, as well as multiple bonds in their molecules [1-2].

Apart from the structural aspects, there are also economic and environmental considerations. Thus, since the whole subject of corrosion is about its destructive economical effect, the used inhibitor must be cheap. Furthermore, due to the recent increasing awareness of green chemistry, it must be a nontoxic and environmentally friendly chemical. One of the sources of these cheap and clean inhibitors is plants.

Green corrosion inhibitors are biodegradable and do not contain heavy metals or other toxic compounds. Some research groups have reported the successful use of naturally occurring substances to inhibit the corrosion of metals in acidic and alkaline environment.

Several reports are available on the various natural products used as green inhibitors. Low-grade gram flour, natural honey, onion, potato, gelatin, plant roots, leaves, seeds, and flowers gums have been reported as good inhibitors.

However, most of inhibitors have been tested on steel and nickel sheets. Although some studies have been performed on aluminum sheets, the corrosion effect is seen in very mild acidic

or basic solutions (mill molar solutions). Many recent researches [3-10] have adopted this trend and carried out their work on naturally occurring substances. Promising results were obtained in previous work in this field.

The objective of this study to investigate the effect of ginger extract as green corrosion inhibitor for the mild steel in 1.0 M HCl at different temperatures by using weight loss ,OCP , linear and Tafel polarization techniques. The effects of temperature were also studied. The evaluation (AEG) against different microorganisms has also been providing by using biocide.

2-EXPERIMENTAL

2.1. Materials

The mild steel specimens tested in the present study are in the form of sheet, the designation and analysis of the material is given in Table (1). Before immersion the obvious electrode in the test solution each of them is prepared by polishing with emery paper from 250 to 1200 grade to obtain a smooth surface, washing with distilled water and then degreased with acetone about 5 minutes, washed again with distilled water then dried using filter papers.

Table (1): Chemical Composition of Mild Steel by Wt %

C	Si	Mn	P	S	Cr	Mo	Ni	Al
0.0826	0.100	0.369	0.0262	0.00791	0.00531	0.00211	0.0163	<0.0001
Co	Cu	Nb	Ti	V	W	Pb	As	Fe
0.000574	0.00375	0.00175	0.00048	0.00251	0.0158	0.00282	0.0123	< 99.35

2.2.Ginger Extraction:

Ginger (*Z. officinal* Roscoe) rhizomes were purchased from the local market . One kilogram fresh ginger rhizome was cleaned, washed under running tap water, cut into small pieces, air dried and powdered. 125 g of this powder were macerated in 1000 ml

of distilled water for 12 h at room temperature and were then filtered. The concentration of the extract is 24 mg/ml [11]

2.2. Evaluation of the effect of biocides (BIOPOL-TC/3) on (AEG):-

2.2.1. Detection and isolation of different microorganisms:-

The pure cultures of different bacteria isolated were identified by conventional bacteriological test methods and by reference to the keys outlined for *Bacillus subtilis* by (Baklola, 2013) [12], *Pseudomonas aeruginosa* by (APHA, 2005) [13], *Escherichia coli* by (Pettibone, 1992) [14], *pseudomonas fluorescens* (Cappuccino and Sherman, 2002) [15] and *Staphylococcus aureus* by (APHA, 2005) [13].

2.2.2. Purification and identification of bacterial isolates:-

Bacterial colonies developed from all previously mentioned media were chosen and picked up according to variation in culture characteristics and colony formation then purified by streak-plate method on nutrient agar medium (Difco) of the following composition (g/liter): Bacto beef extract; 3.0, Bacto Peptone; 5.0, Bacto agar; 15.0, Distilled water; 1.0 liter. Pure isolates were maintained on slants of the same medium at 4°C for subsequent identification. Almost all microscopical examinations and biochemical testing used for identification were carried out according to Collins and Lyne and Cheesbrough (1984) [16-17]

2.2.3. Biocides TC/3 Applications and doses:

BIOPOL-TC/3 is an excellent in-can preservative for dispersion paints, dispersion plasters, polymer dispersions, glues, adhesives and sealants. The optimum dose of BIOPOL-TC/3 as preservative should be determined by the means of recommended doses between 0.05 % and 0.25% depending on application.

2.3. Adopted techniques.

A- Weight loss measurements.

Weight loss measurements were carried out by weighing the mild steel specimens before and after immersion in 500 cm³ acid solutions for different time intervals in the presence and absence of various concentrations of (AEG). Experiments were also performed at temperature range (298-328K) in HCl solutions. Duplicate experiments were performed in each case and the mean value of the weight loss was determined.

The corrosion rate (C.R.), the inhibition efficiency (IE %) and the surface coverage (θ), that represents the weight of metal surface covered by inhibitor molecules, was calculated using the following equations:

$$I.E. \% = [1 - (C.R.)_{inh} / (C.R.)_{free}] \times 100 \quad (1)$$

$$\theta = [1 - (C.R.)_{inh} / (C.R.)_{free}] \quad (2)$$

B- Open circuit potential measurements (OCP).

The potential of the mild steel electrode (working electrode) was measured against saturated calomel electrode (SCE) (reference electrode) in 1.0 M HCl solution in absence and presence of different concentrations of the inhibitor.

C- Potentiodynamic polarization measurements.

The electrochemical cell used in potentiodynamic polarization consists of (three electrodes), working electrode (mild steel), reference electrode (saturated calomel electrode (SCE)) and platinum wire used as counter electrode. The exposed area of working electrode to solution was (1 cm²). For the anodic and cathodic potentiodynamic polarization (Tafel plots) the entire potential scan was programmed to take place within ± 250 mV of the corrosion potential. The measurements were conducted at scanning rate of 0.2 mV/s.

D- Surface Examinations Techniques:

I- Scanning Electron Microscope (SEM):

The scanning electron microscope (SEM) is a type of electron microscope giving images of the sample surface by scanning it with a high-energy beam of electrons in a raster scan pattern.

SEM images should confirm the electrode surface. The specimens have been rinsed before and after immersion in different solutions.

II- Energy Dispersive X-ray Analysis (EDAX):

(EDAX) is an analytical technique used for the elemental analysis or chemical characterization of a sample. The identification of the elements present in the surface of specimens before and after immersion in different solutions will be performed using an energy dispersion X-ray analysis. This technique is used in conjunction with SEM.

3- Results and discussion

3.1.1. GC/MS give light on the structure of Gingerol compound (Fig 1) which is obtained from the extraction of ginger [18]. The GC/MS spectrum of Gingerol exhibits one peak at m/z = 137 as the molecular peak where the retention time 25.873 minutes. (Fig 2).

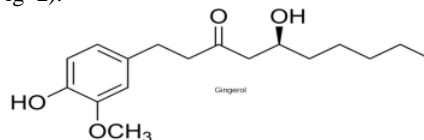


Fig (1) The structure of Gingerol .

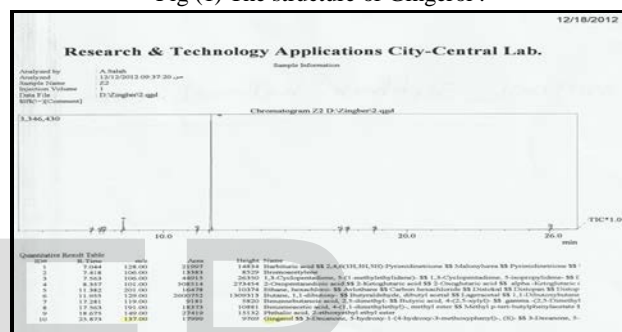


Fig. (2) GC/MS Scan of ginger extract.

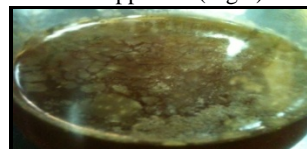
3.1.2. Evaluation of the stability and antimicrobial activity of Ginger extract in different temperatures.

The aim of the following experiment is to test the efficiency of TC/3 (anti-bacterial agent) over the natural product extract (AEG) in different doses (0.05 and 0.25%) and temperatures (25 and 60°C).

BIOPOL-TC/3 has shown its effectiveness against the following bacterial microorganisms among others: (*Bacillus subtilis*, *Pseudomonas aeruginosa*, *Escherichia coli*, *pseudomonas fluorescens* and *Staphylococcus aureus*). In the case of using water as a medium for ginger extract, microbial activity presence is a must. Where we tested the ginger extract with water in the presence and absence of TC/3 (anti-bacterial agent) at 25 and 60°C. Three vials were prepared, containing 1 gm/100 ml H₂O, the following results were obtained:

1- In the absence of TC/3, microbial contamination appeared on the surface of the extract within 2-4 days at 25°C. But in presence of low and high doses of TC/3 no microbial contamination appeared for 12 months.

2- Moreover at 60°C, in both cases of low and high doses of TC/3 no microbial contamination appeared. (Fig.3).



No dose

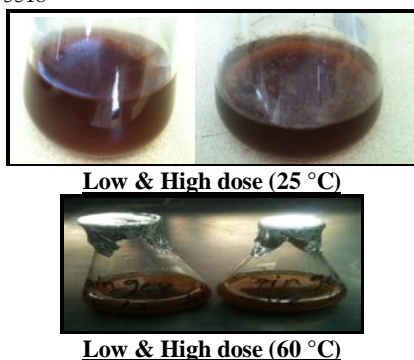


Fig (3) Effect of biocides (BIOPOL-TC/3) on Ginger extract by using low and high dose at 25°C and 60°C .

3.2. Electrochemical Techniques

3.2.1. Open Circuit Potential (OCP) Measurements:

The way in which a metal changes its potential upon immersion in solution indicates the nature of reaction taking place at its surface. Whilst a shift in potential in the noble direction denotes film repair and healing, a shift in the negative direction signifies film destruction and the exposure of more of the surface electrodes to the aggressive solution. The results obtained were used in discussion the mechanism of oxide film growth in aerated test solutions.

The (OCP) for mild steel as a function of time in 1.0 M HCl in absence and in the presence of different concentrations of all under testing aqueous extract of ginger are studied.

As revealed from inspection of curves (Fig.4) and the results are listed in table(2), the potential of the mild steel electrode is measured directly after immersion as the steady state potential varies with different concentrations of the used (AEG) solutions (0.01-5.0g. %). In aqueous extract of ginger, there is always a general tendency for the OCP to drift with time towards more stable values at which it tends to be stabilized after 30 minutes. Inspection of OCP curves reveals that . There is always a general tendency for the immersion potential (E_{im}) to shift from negative to the positive direction. The values of steady state potential (E_{ss}) in this case are higher than the value in free acid.

Table (2). Values of E_{im} and E_{ss} (mV) for mild steel in 1.0 M HCl at different concentrations of AEG.

Media	CONC. %	E_{im} (mv)	E_{ss} (mv)
HCl (blank)	1.0M	-468	-484
GINE	0.01	-462	-464
	0.1	-447	-456
	1.0	-444	-445
	2.5	-440	-435
	5.0	-439	-415

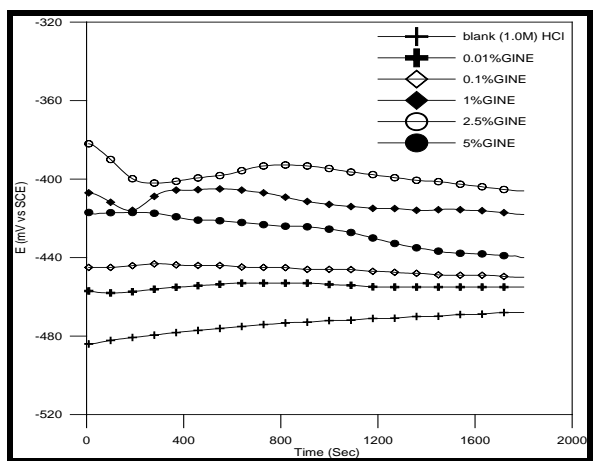


Fig.(4). Potential-time curves for mild steel in GINE at conc.5% at 1.0M HCl

3.2.2. Potentiodynamic Polarization Measurements

Fig. (5) represents linear and Tafel polarization curves of 1.0M HCl in different concentrations(0.01-5.0g. %) of (AEG) at room temperature.

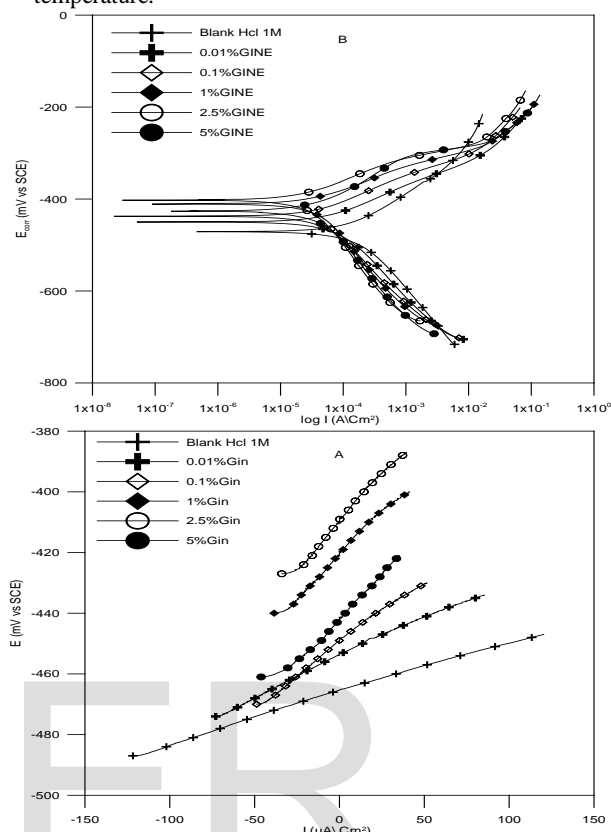


Fig. (5). Linear (A) and Tafel plots (B) polarization curves of mild steel in GINE at conc. 5% at 1.0M HCl

The corrosion kinetic parameters are tabulated in Table (3), showing that the polarization resistance (R_p), Tafel slopes constants (β_a , β_c), corrosion potential (E_{corr}), corrosion current density (I_{corr}), corrosion rate (C.R.) and inhibition efficiencies (I.E.%) are function of the of different concentrations (AEG).

Table (3): Polarization parameters for mild steel in 1.0M HCl at different concentrations of AEG.

Test Solution	Conc v/v%	R_p Ω	Tafel Slopes		E_{corr} (mV)	I_{corr} $\mu A/Cm^2$	C.R (mpy)	I.E (%)
			β_a (mV/decade)	β_c (mV/decade)				
HCl 1.0M	-	180	124.5	187.6	471	225.3	207.73	-
GINE	0.01%	262	72.84	141.2	449.9	70.37	64.88	69
	0.1%	427	69.28	146.8	437.5	46.2	42.60	79
	1%	496	62.22	183.1	410.8	41.09	37.89	82
	2.5%	506	62.51	168.9	402.5	26.12	24.08	88
	5%	508	64.12	137.2	426.2	24.12	22.24	89

An inspection of the results presented in Fig. (5) and Table (3) reveals that, increasing the concentration of the additive (AEG).shows the following:

- It is clearly that different concentrations of (AEG) shifted both anodic and cathodic branches of polarization curves to

lower values of current density indicating that all concentration act as mixed type inhibitors. The addition of different concentration of (AEG) to HCl solution reduces the anodic dissolution of mild steel and also retards the cathodic hydrogen evolution reaction.

- (ii) The corrosion potential (E_{corr}) shifted slightly to more positive values while the corrosion current (I_{corr}) decreases with increasing the inhibitor concentration, indicating the inhibiting effect of these compounds.
- (iii) The variable values of the cathodic Tafel slopes suggest that the inhibition action of (AEG) such compounds occurs by simple blocking of the electrode surface area [19].
- (iv) The obtained results indicated that (AEG) compounds inhibit HCl corrosion of mild steel via their adsorption on both anodic and cathodic active sites without modifying the mechanism of corrosion reaction. This means that the adsorbed inhibitor molecules block the surface active sites and decrease the area available for hydrogen evolution and metal dissolution reactions [20].
- (v) The (I.E.%) calculated was found to increase with increasing the AEG. concentration.

3.3 Weight Loss Measurements:-

Weight loss measurements were carried out for mild steel in 1.0M HCl in the absence and presence of different concentrations of AEG. It is noted that the IE% increases steadily with increasing the concentration of AEG and decrease with rising the temperature from 298-328 K. The inhibition efficiency (IE%) and surface coverage (θ) were calculated by equations (1,2).

3.3.1. Thermodynamic and Adsorption Considerations:

To investigate the mechanism of inhibition and to determine the activation energy of the corrosion process, weight loss of mild steel in 1.0 M HCl was determined at various temperatures (298-328 K) in the absence and presence of different concentrations of AEG.

In an acidic solution the corrosion rate is related to temperature by the Arrhenius equation [21]:

$$\log C.R. = [-E_a / 2.303 RT] + \log A \quad (3)$$

Where (C.R.) is the corrosion rate, E_a is the apparent activation energy, R is the molar gas constant, T is the absolute temperature and A is the frequency factor. Fig. (5) shows the plot of $\log C.R.$ versus $1/T$. Linear plots were obtained for different AEG compounds. The values of E_a were computed from the slope of the straight lines and are listed in Table (4). It is clear from this table that E_a values in presence of the AEG are higher than in their absence. Inspection of these data reveals that the apparent activation energy E_a in HCl in the absence of AEG was $46.886 \text{ kJ/mol}^{-1}$.

Table (4): Activation parameters for mild steel in 1.0 M HCl in the absence and presence of different concentrations of Ginger.

Systems	Conc. (w/v) %	E_a	ΔH^*	ΔS^*
BLANK	0	46.886	44.288	-112.755
Ginger	5	49.421	46.823	-109.251
	2.5	49.546	46.948	-108.864
	1	49.671	47.073	-108.475
	0.1	49.462	46.864	-108.777
	0.01	49.079	46.481	-109.552

Low activation energy means fast reaction and high activation energy means slow reaction. High activation energy corresponds to a reaction rate that is very sensitive to temperature. Conversely small activation energy indicates a reaction rate that varies only slightly with a temperature. If reaction has zero activation energy, its rate is independent of temperature. In some cases, activation energy (E_a) is found negative which indicates

that the rate decreases when temperature is raised and such behaviour is a signal that reaction has a complex mechanism [22,23]. Enthalpy and entropy of activation ΔH^* and ΔS^* were obtained by applying the transition state equation:

$$C.R. = [RT/Nh] \exp(\Delta S^*/R) \exp(-\Delta H^*/RT) \quad (4)$$

$$\log C.R. = \log[RT/Nh] + (\Delta S^*/R) - (\Delta H^*/RT) \quad (5)$$

Where h is the Planck's constant, N is the Avogadro's number, T is the absolute temperature and R is the universal gas constant. Plots $\log[C.R./T]$ as a function of $1/T$ were made in Fig. (6). Straight lines were obtained with a slope of $(-\Delta H^*/RT)$ and an intercept of $\log[R/Nh] + (\Delta S^*/R)$, being the values of ΔH^* and ΔS^* calculated, and listed in Table (4). While an endothermic adsorption process ($\Delta H^* > 0$) is attributed unequivocally to chemisorption, an exothermic adsorption process ($\Delta H^* < 0$) may involve either physisorption or chemisorption or a mixture of both processes [50]. In the present work, the positive sign of the activation enthalpy (ΔH^*) reflects the endothermic nature of the steel dissolution process and that the dissolution of steel is difficult. The order of the phenomena ascribed by the negative values of (ΔS^*), may probably be explained by the possibility of the formation of iron complex on the metal surface [24].

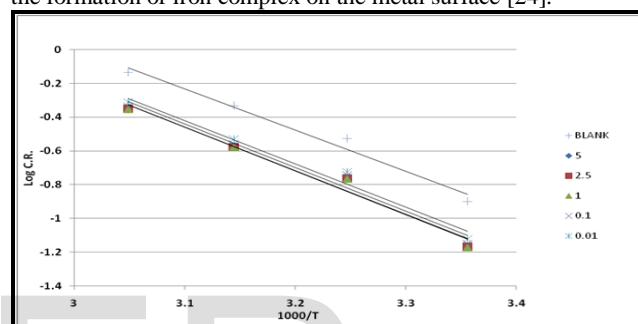


Figure (6): Arrhenius plots for mild steel in 1.0 M HCl in the absence and presence of different concentrations of Ginger.

In order to get a better understanding of the adsorption mode of the inhibitor on the metal surface, the data were tested graphically by fitting them to various isotherms to find the best isotherm which describes this study. The value of correlation coefficient (R^2) was used to determine the best fit isotherm. Langmuir adsorption isotherm was found to fit well the experimental data. According to this isotherm, θ is related to the C and adsorption equilibrium constant K_{ads} , via the following equation [25].

$$C/\theta = [1/K_{\text{ads}}] + C \quad (6)$$

Using equation (6), plots of $\log(C/\theta)$ versus C gave straight lines Fig. (7), with a slope of around unity confirming that the adsorption of different AEG on mild steel surface in hydrochloric acid solution obeys the Langmuir adsorption isotherm at 25°C (similar data are obtained at different temperatures). The values of Langmuir adsorption parameters obtained from the plots are recorded in Table (4). The results show that the slopes and R^2 values are very close to unity indicating strong adherence of the adsorbed inhibitors to the assumptions of Langmuir [26].

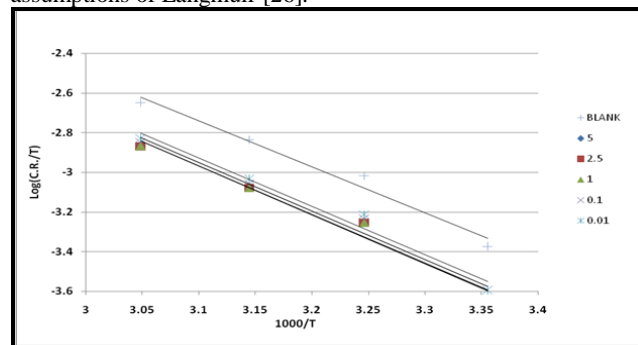


Figure (7): Alternative Arrhenius plots for mild steel dissolution in 1.0 M HCl in the absence and presence of different concentrations of Ginger.

The equilibrium constant of adsorption obtained from the slopes of the Langmuir isotherms was used to calculate the free energy for the adsorption of different AEG on the surface of mild steel. The free energy of adsorption of different AEG on the metal surface is related to the equilibrium constant of adsorption according to equation (7):

$$K_{ads} = [1/55.5] \exp(-\Delta G_{ads}/RT) \quad \dots\dots\dots (7)$$

Where R is the universal gas constant, ΔG_{ads} is the free energy of adsorption and 55.5 is the concentration of water in solution (mol L^{-1}) [27].

The enthalpy and entropy of adsorption (ΔH_{ads} and ΔS_{ads}) can be calculated using equation (8).

$$\ln K_{ads} = [\ln 1/55.5] - (\Delta H_{ads}/RT) + (\Delta S_{ads}/R) \quad \dots\dots\dots (8)$$

Using equation (8), the values of ΔH_{ads} and ΔS_{ads} were evaluated from the slope and intercept of plot $\ln K_{ads}$ versus $1/T$, Fig. (8). The values of ΔG_{ads} , ΔH_{ads} and ΔS_{ads} are listed in Table (5). From the results, it is significant to note that the calculated values of ΔG_{ads} are negative indicating that the adsorption is a spontaneous process. Generally, the values of ΔG_{ads} around -20 kJ mol^{-1} or lower are consistent with the electrostatic interaction between charged molecules and the charged metal surface (physisorption), while those around -40 kJ mol^{-1} or more negative involve chemisorption [28]. In the present study, the values of ΔG_{ads} ranged from $(-35.18 \text{ to } -35.64)$ at temperatures ranged from (25 to 55 °C), which probably means that both physisorption and chemisorption are taking place.

Table (5): Thermodynamic parameters for adsorption of Ginger in 1.0 M HCl at different temperatures from Langmuir adsorption isotherm

Natural Product	Tem., K	R ²	K _{ads} ,	ΔG _{ads} ,	ΔH _{ads} ,	ΔS _{ads} ,	
			L mol ⁻¹	kJ mol ⁻¹	kJ mol ⁻¹	J mol ⁻¹ K ⁻¹	
Ginger	298	0.996	26406.23	-35.18	-22.7417923	0.0388091	a
	308	0.997	23209.79	-36.03			
	318	0.997	38534.20	-38.54	-22.7376209	103.0635284	b
	328	0.997	8520.80	-35.64			
(a)	values obtained from Eq. (8)			(b) values obtained from Eq. (9)			

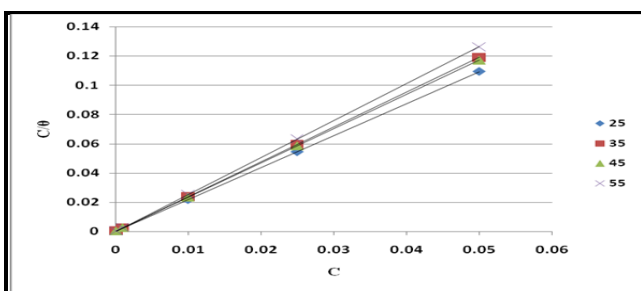


Figure (8): Langmuir adsorption isotherm for Ginger on mild steel in 1.0 M HCl at different temperatures.

The values of ΔS_{ads} are positive in the adsorption process and this could be explained as follows:

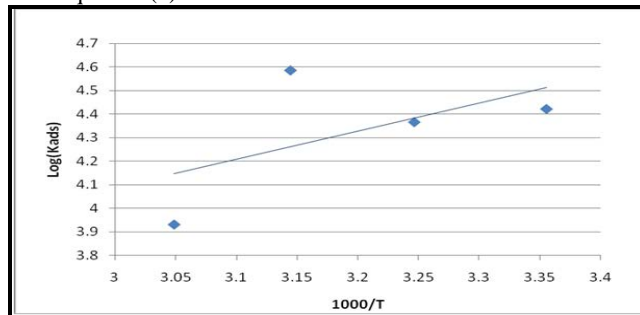
The thermodynamic values which are obtained the algebraic sum of the adsorption of organic molecules and desorption of water molecules [29], therefore, the gain in enthalpy is attributed to the increase in solvent entropy [29,30]. The values of ΔH_{ads} provides further information about the mechanism of

corrosion inhibition. The endothermic adsorption process is ascribed unambiguously to chemisorption and an exothermic process may involve either physisorption or chemisorption or a combination of both [31]. In the present study, the negative values of ΔH_{ads} obtained indicate a combination of both physisorption and chemisorption processes.

The values of ΔH_{ads} and ΔS_{ads} can also be calculated by using the following equation [32]:

$$\Delta G_{ads} = \Delta H_{ads} - T \Delta S_{ads} \quad \dots\dots\dots (9)$$

Using equation (9), the plot of ΔG_{ads} versus T gives a straight line (Fig. (9)) with a slope of $-\Delta S_{ads}$ and intercept of ΔH_{ads} . The values obtained are well correlated with those obtained from equation (8)



Fig(9) Plot of log K_{ads}. Versus 1/T x10³ for AEG

3.4. Surface Morphology of the Metal Electrodes.

The scanning electron microscope images and energy dispersive X-ray analysis further supported the formation of a surface film by the inhibitors and their interaction with surface atoms of mild steel.

3.4.1. Scanning Electron Microscope (SEM) Analysis

Fig (10 A) illustrates the morphology of the surface of polished mild steel electrode before exposure to corrosion media (blank). The specimens were subjected to microscopic examination at x 1500. The micrograph shows a characteristic inclusion, which was probably an oxide inclusion. Fig (10 B) shows SEM image of the surface of the studied mild steel electrode specimen after immersion in 1.0 M HCl solution for 24 hr. The micrograph reveals that, the surface was strongly damaged. The corroded areas are shown as black grooves in the specimen with gray and white zones, which correspond to the dandruff of iron oxide. It suggested an uncovered surface of metal electrode severally corroded. The highly oxidized phase perhaps formed in air when desiccated under no protection for the surface.

Fig (10 C) show SEM images for the surface of another mild steel specimen after immersion for the same time interval in 1.0 M HCl solution containing 1.0×10^{-3} ginger extract. The micrograph reveals that, the inhibited metal surface is smoother than the uninhibited surface, a good protective film present on the metal surface. This confirms the highest inhibition efficiency of the inhibitors.

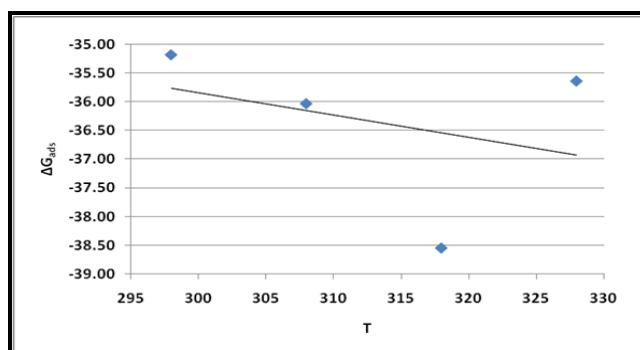


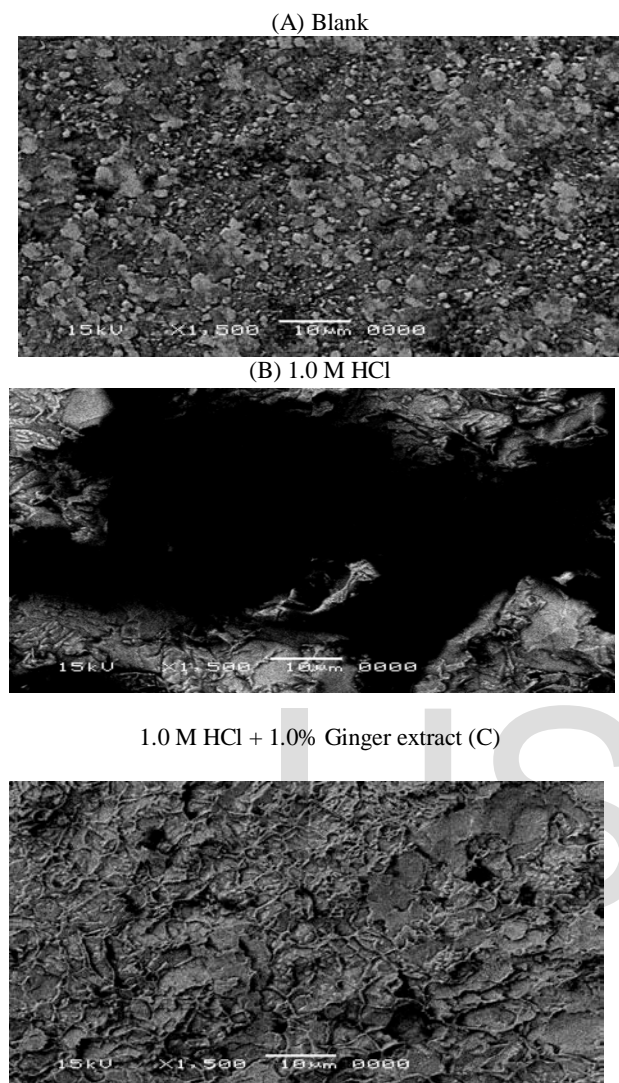
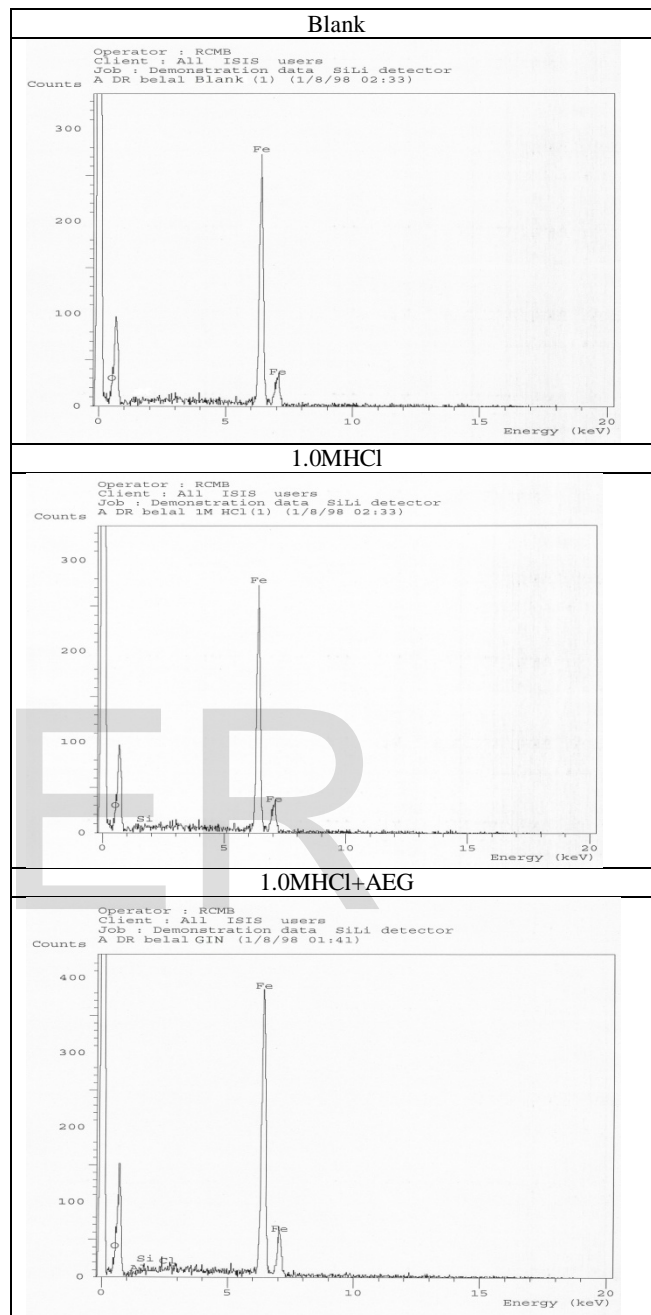
Figure (10): plot of ΔG_{ads} versus absolute temperature for AEG.

Fig (10): (A) SEM image of polished mild steel surface.
 (B) SEM image of mild steel exposed to 1.0 M HCl.
 (C) SEM image of mild steel exposed to 1.0 M HCl having 1.0% Ginger extract

3.4.2. Energy Dispersive X-ray Analysis (EDAX)

It is important to take into consideration the percentage of the elements present on the surface of the mild steel. The EDAX analysis of the surface reveals the presence of oxygen and iron, suggesting therefore the presence of iron oxide / hydroxide table (6) and (Fig (11)). The presence of the peaks of carbon, nitrogen, chloride, silicon and sulphur is explained by the adsorption of the inhibitor (AEG) on the products of corrosion of the mild steel.



Fig(11) EDAX examination of the area of mild steel which represents (A) Blank (B) immersed in 1.0 M HCl for 24 hr.(C) immersed in 1.0 M HCl in the present of AEG for 24 hr

Table (6): Chemical composition of mild steel by using EDAX spectra

specimen	Fe %		O %		Cl %		Si %		Al %		N %	
	Element	Atomic	Element	Atomic	Element	Atomic	Element	Atomic	Element	Atomic	Element	Atomic
	%	%	%	%	%	%	%	%	%	%	%	%
Pure mild steel	99.25	95.82	0.75	4.28	---	---	---	---	---	---	---	---
Mild steel in (1.0 M HCl)	94.01	82.33	5.51	16.83	---	---	0.48	0.84	---	---	---	---
Mild steel in (1.0 M HCl + Gin.)	94.573	84.743	4.593	13.773	---	---	0.367	0.660	0.467	0.837	---	---

CONCLUSION:

From the overall experimental results the following conclusion can be deduced:

- 1- In the absence of biocide, microbial contamination appeared on the surface of the extract within 2 - 4 days at 25°C. But in presence of low and high doses of TC/3 no microbial contamination appeared for 12 months.
- 2-The AEG shows good performance as corrosion inhibitor in 1.0 M HCl.
- 3-The inhibition efficiency increases with increase in the concentration of AEG, but decreases with an increase in temperature.
- 4- the AEG influences both the cathodic and anodic reactions in the HCl solution. This indicates that the additive acts as mixed-type inhibitors.
- 5- The AEG inhibits the corrosion by getting adsorbed on the metal surface following Langmuir adsorption isotherm.

REFERENCES

1. Sastri V.S. Green Corrosion Inhibitors. Theory and Practice. John Wiley & Sons Hoboken, NJ; 1998.
2. Sastri V.S. Corrosion Inhibitors Principles and Applications. John Wiley & Sons: New York; 1998.
3. El-Etre, A. Y. J. Colloid Interface Sci. 2007, 314, 578.
4. El-Etre, A. Y. Appl. Surf. Sci. 2006, 252, 8521.
5. Benabdellah, M.; Benkaddour, M.; Hammouti, B.; Bendahhou, M.; Aouniti, A. Appl. Surf. Sci. 2006, 252, 6212.
6. Chaieb, E.; Bouyanzer, A.; Hammouti, B.; Benkaddour, M. Appl. Surf. Sci. 2005, 246, 199.
7. Müller, B. Corros. Sci. 2002, 44, 1583.
8. Li, Y.; Zhao, P.; Liang, Q. Hou, B. Appl. Surf. Sci. 2005, 252, 1245.
9. El-Etre, A. Y.; Abdallah, M.; El-Tantawy, Z. E. Corros. Sci. 2005, 47, 385.
10. Bouyanzer, Hammouti, B.; Majidi, L. Mater. Lett. 2006, 60, 2840.
11. Saber A. Sakr and Somya Y. Shalaby. Journal of Applied Pharmaceutical Science 01 (10) (2011) 36-42.
12. Baklola, E. A. The impact of sanitary and food industrial wastes on water quality of Menyat Samanoud agriculture drain at El-Dakahlia Governorate., Egypt, Fac. Sci., Tanta., Univ., M. Sc. Thesis. (2013).
- 13- American Public Health Association "APHA". Standard Methods for the Examination of Water and Wastewater (21st ed.), Washington, D. C. (2005)
- 14- Pettibone, G. W. The use of lauryl treptose broth containing 4-methyl umbelliferyl- beta- D-glucuronide "MUG" to enumerate *E.coli* form fresh water sediment. Lett. Appl. Microbiol. 15(5)(1992)190-192.
- 15- Cappuccino, J.G. and Sherman, N. Microbiology: A laboratory manual. 6th ed. Benjamin Cummings, San Francisco.(2002)
- 16-Collins, C.H. and Lyne, P.M. Microbiological methods. 5th Ed. 450, Butterworth, England.(1984)
- 17-Cheesbrough, M. "Microscopical examination of specimens" and "Biochemical testing of microorganisms", in: Medical laboratory manual for tropical countries. Tropical health technology, Butterworth-Heinemann Ltd. Printed in Great Britain at University press, Cambridge, 2(1984).26-39 and 58-69.
- 18- Yitao, Wenkuili, Wenzhong, L., and Richard, B. VAN, B. J Agric Food Chem. Nov 11; 57(21)(2009) 10014–10021.
- 19-M. Vracar Lj and D.M. Dragic. Corros. Sci. 44 (2002) 1669.
- 20-B. El-Mahdi, B. Memari, M. Traisnel, F. Bentiss and M. Lagrenee. Mater. Chem. Phys. 77 (2002) 489.
- 21-E.E. Ebenso, H. Alemu, S.A. Umoren and I.B. Olet. Int. J. Electrochem. Sci. 3, (2008) 1325-1339.
- 22-E.E. Ebenso, H. Alemu, S.A. Umoren and I.B. Obot. Int. J. Electrochem. Sci. 3,(2008) 1325-1339.
- 23-S.A. Umoren and E.E. Ebenso. Pigment and Resin Technol. 37 (8) (2008) 173.
- 24-M.Y. Mourad, S.A. Seliman and S.M. Abd El-Metaal. Bull. Soc. Chim. Fr. 128, (1991) 832- 836.
- 25-I. Langmuir, J. Am. Chem. Soc. 39 (1947) 1848-1850.
- 26-S.A. Ali, M.T. Saeed and S.U. Rahman. Corros. Sci. 45 (2005) 253.
- 27-E. Khamis. Corrosion. 46 (1990) 476-484.
- 28-E. Bensajjay, S. Alehyen, M. El-Achouri and S. Kertit. Anti-Corros. Meth. Mater. 50 (2003) 402.
- 29-E.T. Kumar, S. Viswanatham and G. Udayabhanu. Corros. Eng. Sci. Technol. 39 (2004) 327.
- 30-B. Ateya, B. El-Anadoul and F. El-Nizamy. Corros. Sci. 24 (1984) 509.
- 31-S.A. Ali, A.M. El-Shareef, R.F. Al-Ghamdi and M.T. Saeed. Corros. Sci. 47 (2005) 2659.
- 37-S.S. ShivaKumar and N.K. Mohana. Int. J. Electrochem. Sci. 7 (2012) 1620-1638.